THE JOURNAL OF PHYSICAL CHEMISTRY A

ARTICLE

pubs.acs.org/JPCA

Structure of 2,4-Diaminopyrimidine−Theobromine Alternate Base Pairs

Zsolt Gengeliczki,[†] Michael P. Callahan,[‡] Martin Kabeláč,[§,#] Anouk M. Rijs,[∥] and Mattanjah S. de Vries*[,⊥]

[†]Department of Chemistry, Stanford University, Stanford, California 94305-5080, United States

[‡]NASA Goddard Space Flight Center, Greenbelt, Maryland 20771, United States

[§]Faculty of Natural Sciences, University of South Bohemia, Branišovská 31, 37005 České Budějovice, Czech Republic

[#]Institute of Organic Chemistry and Biochemistry, Academy of Sciences of the Czech Republic, v.v.i, Center for Biomolecules and Complex Molecular Systems, Flemingovo nám. 2, 166 10 Prague 6, Czech Republic

[∥]FOM Institute for Plasma Physics Rijnhuizen, Edisonbaan 14, 3439 MN Nieuwegein, The Netherlands

[⊥]Department of Chemistry and Biochemistry, University of California Santa Barbara, California 93106-9510, United States

Supporting Information

ABSTRACT: We report the structure of clusters of 2,4-diaminopyrimidine with 3,7-dimethylxanthine (theobromine) in the gas phase determined by IR-UV double resonance spectroscopy in both the near-IR and mid-IR regions in combination with ab initio computations. These clusters represent potential alternate nucleobase pairs, geometrically equivalent to guanine−cytosine. We have found the four lowest energy structures, which include the Watson−Crick base pairing motif. This Watson−Crick structure has not been observed by resonant two-photon ionization (R2PI) in the gas phase for the canonical DNA base pairs.

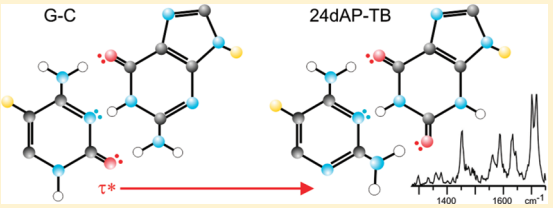

INTRODUCTION

The study of nucleobases and base pairs in isolation in the gas phase makes it possible to observe their intrinsic properties, distinct from properties induced by their biological environment such as the solvent or the macromolecular structure.[1] One great advantage of gas phase studies is the possibility to obtain isomer selective information, such as the dependence of properties on the tautomeric form or on specific structures. One example is the excited state dynamics, which we have found to depend strongly on the structural and tautomeric details of nucleobases and base pairs.[2−4] The UV excited states of the canonical bases (A, G, C, T, and U) generally decay in less than 1 ps, orders of magnitude faster than in other heterocyclic compounds and in even closely related structures including tautomers.[4] Theoretical models describe the pathway as internal conversion via conical intersections, thus avoiding photochemical damage following UV absorption.[5] This is an intriguing observation because avoidance of photochemistry would have been highly advantageous for the first self-replicating molecules in prebiotic times before modern enzymatic repair and before the formation of the ozone layer that later attenuated the high levels of UV radiation on the early Earth.[6,7] This suggests the possibility that the natural bases were chemically selected in part due to their high intrinsic photostability and that this functionality is preserved from a prebiotic world. Electronic excited states are affected by the formation of clusters, and therefore the excited state dynamics of base pairs depends on their specific structure. In the case of the canonical bases in the gas phase, we found the biologically most relevant structure of GC to have the shortest-lived excited state,[2] and we found the same for the biologically most relevant structures of GG and CC pairs.[8−10]

Numerous studies have proposed possible alternate base pair combinations that could suggest credible alternatives to the canonical base pairing scheme in terms of stability and recognition.[11] Benner and co-workers, for example, have proposed an "alternate genetic lexicon" formed by merely exchanging the hydrogen donor and acceptor groups in the base pair structures.[12] One such combination is xanthine paired with 2,4-diaminopyrimidine (24daP), which forms a geometrically identical replacement for guanine−cytosine (GC). If the canonical bases were present in a primordial soup, it is reasonable to assume that all other derivatives and analogues were present as well.[13] Furthermore, biological evolution presumably takes place only when a genetic recognition mechanism is in place, such that the original selection of the genetic building blocks would have been the result of a prebiotic chemical evolution. Therefore, a comparison of the characteristics of all possible nucleobase compounds may shed light on functional differences that may have played a role in early chemistry. These considerations motivate us to expand our investigations of the pairing characteristics of nucleobases to alternate base pairs, of which this study presents a first example.

24daP and theobromine (TB) can form an alternate base pair that is geometrically identical to G-C, as shown in Figure 1. We used TB, which is 3,7-dimethylxanthine, to represent xanthine in this alternate base pair. The methyl blocking leaves only one NH

Special Issue: Pavel Hobza Festschrift

Received: June 21, 2011
Revised: August 17, 2011

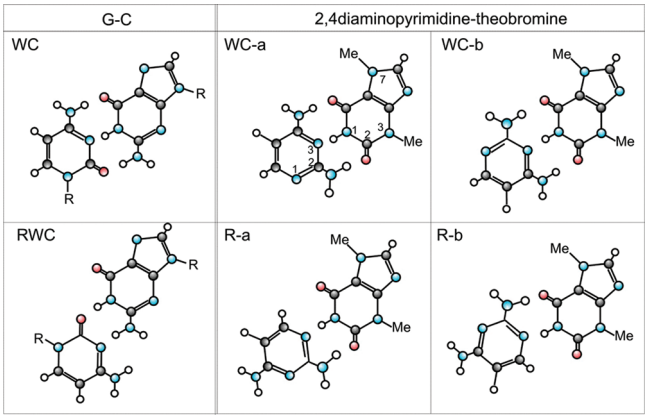

Figure 1. The four lowest energy structures of the 24daP−TB cluster, compared to the WC and reverse WC structures of the canonical GC base pair. "Me" indicates methyl group; "R" indicates the site for the sugar−phosphate connection. The numbering scheme is indicated in the WC-a structure.

position available for hydrogen bonding, reducing the number of possible structures. Even with this simplification, a fair number of structures is still possible, as will be discussed below. Importantly for this study, the N1 position is not blocked, allowing, among others, the Watson−Crick (WC)-like structure with the NH_2 and C═O groups exchanged between bases, (see Figure 1).

METHODS

Computational. To ensure that we did not overlook any energetically important structure, we explored the potential energy surface of 24daP−TB complexes with a molecular dynamics/quenching (MD/Q) technique, employing the PM6 semiempirical method with an improved dispersion term.[14,15] We performed these MD/Q simulations at a constant total energy corresponding to an average temperature of 700 K, which is sufficient to overcome the energy barriers between the conformations of the complex. As we will discuss below, we selected the four most stable H-bonded, and two most stable stacked and T-shaped structures for more precise ab initio calculations. We fully optimized these structures and calculated Gibbs free energies and calculated the harmonic frequencies, scaled by a factor of 0.957, at the MP2/cc-pVDZ level of theory with the Gaussian 09 program package.[16] For the calculations of Gibbs free energies, we used the standard ideal gas-rigid rotor−harmonic oscillator approximation.

We determined the interaction energies (all BSSE-corrected) for the optimized geometries as a sum of the complete basis set limit (CBS) of resolution-of-identity (RI-)MP2 energies and evaluated a ($\Delta E_{MP2.5}$) correction term with a standard split-valence 6-31G basis set of atomic orbitals with an added set of diffuse functions of exponent 0.25 on the second row of elements (6-31G (0.25)). Such a basis set can properly describe both the dispersion and stacking interaction with low computational cost.[17] The CBS of RI-MP2 energies was determined by two-point Helgaker's extrapolation[18] using aug-cc-pVXZ basis sets for X = T and Q. The correction term $\Delta E_{MP2.5}$ was calculated according to an equation $\Delta E_{MP2.5} = E(MP2) + (1/2)E^{(3)}$, where $E^{(3)}$ is the third-order MP correlation energy correction. The interaction energies of noncovalent complexes calculated employing this procedure should agree very well with the computationally much more demanding CCSD(T)/CBS data, as shown by Pitoňák et al.[19] All ab initio calculations of interaction energies were carried out using the MOLPRO program package.[20]

Experimental Section. All measurements were performed with an apparatus described in detail elsewhere.[21] In brief, a mixture of 24daP and TB powder is applied to the surface of a sanded graphite bar and placed directly below the orifice of a pulsed valve. The sample is vaporized using a focused Nd:YAG laser (1064 nm, <1 mJ per pulse, 10 ns pulse duration) and cooled in an expanding argon jet (backing pressure 4 bar). Clusters are formed in the expansion region of the jet. The molecules then pass through a 1 × 3 mm rectangular skimmer into the interaction chamber of a reflectron time-of-flight mass spectrometer where they are intersected with IR and UV laser beams.

Tunable UV radiation is produced by a Nd:YAG-pumped dye laser (10 Hz, ∼2 mJ per pulse at probe wavelengths, 0.03 cm^{-1} bandwidth), and ions are created by two photon ionization. Resonance enhanced multi-photon ionization (REMPI) spectra are recorded by monitoring mass selected peaks while tuning the two photon, one color excitation-ionization wavelength. IR-UV double resonance spectra are recorded with two laser pulses delayed in time by ∼400 ns. The first pulse serves as a "burn" pulse, which removes the ground state population and causes depletion in the ion signal of the second "probe" pulse, provided both lasers are tuned to a resonance of the same isomer.

Near-IR "burn" frequencies ranging from 3100 cm^{-1} to 3800 cm^{-1} (intensity 10−12 mJ per pulse, 3 cm^{-1} bandwidth) are produced in an optical parametric oscillator/amplifier (OPO/OPA) setup (LaserVision) pumped by the fundamental output of a Nd:YAG laser. Mid-IR radiation is provided by the free electron laser FELIX in The Netherlands, which produces a 5 μs train of picosecond laser pulses, tunable between 40 and 2000 cm^{-1} and with a bandwidth of approximately 0.5% of the central frequency (full width at half-maximum (fwhm)).[22,23] In the present experiments, which were carried out in a similar molecular beam apparatus,[24] the range from 750 to 1900 cm^{-1} was used with energies of up to 100 mJ per macro pulse.

RESULTS AND DISCUSSION

We first considered 20 possible planar cluster structures, at a lower level of theory (B3LYP/6-311+G(d,p).[25] These structures are given in Supporting Information Table S1 and include combinations with different tautomeric forms of 24daP and TB. The two lowest energy structures are WC-a and WC-b, which are within 0.11 kcal/mol of each other. The next higher energy structures are R-a and R-b at 1.7 and 1.8 kcal/mol, respectively. Furthermore, nine of these structures are from 13 to 45 kcal/mol higher in energy, while five others converge to lower energy structures upon optimization. These 14 structures will not be considered further. Finally, two ionic structures appeared at about 5 kcal/mol, but their IR frequencies (given in Table S2) mismatch experimental results completely, and so these two structures will also not be considered further.

We further optimized the four lowest energy structures given schematically in Figure 1, as well as a pair of stacked structures (S1, S2) and a pair of T-shaped structures (T1, T2), shown in Figure 2. At the higher level of theory, the relative energies are slightly different, but they remain at the same relative order and well within the same order of magnitude. The calculated interaction energies (see Table 1) show that there is an energy gap of

dx.doi.org/10.1021/jp205831n |J. Phys. Chem. A XXXX, XXX, 000–000

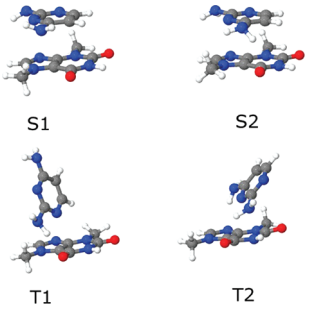

Figure 2. Stacked and T-shaped structures of the 24daP−TB alternate base pair.

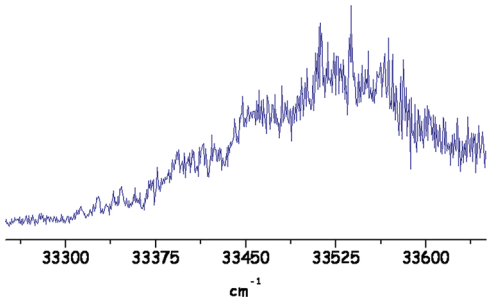

Figure 3. The one-color R2PI spectrum of the TB+24daP cluster.

Table 1. Interaction Energies (in kcal/mol) of the Examined Systems

	AVTZ[a]	AVQZ[b]	CBS[c]	$\Delta E_{MP2.5}$[d]	ΔE_{tot}[e]	ΔG_{tot}[f]
WC-a	−18.26	−18.91	−19.37	0.16	−19.21	−6.90
WC-b	−18.31	−18.98	−19.45	0.22	−19.23	−6.32
R-a	−16.20	−16.75	−17.14	0.25	−16.89	−4.85
R-b	−15.81	−16.36	−16.74	0.23	−16.51	−4.42
T1	−11.32	−11.70	−11.97	1.35	−10.62	1.23
T2	−11.73	−12.19	−12.53	1.79	−10.74	1.39
S1	−15.49	−16.08	−16.49	3.73	−12.76	1.42
S2	−14.21	−14.74	−15.13	3.73	−11.40	2.26

[a] BSSE corrected interaction energies calculated at the RI-MP2/aug-cc-pVTZ//MP2/cc-pVDZ level. [b] BSSE corrected interaction energies calculated at the RI-MP2/aug-cc-pVQZ//MP2/cc-pVDZ level. [c] CBS extrapolated interaction energies from the previous two values. [d] The correction term $\Delta E_{MP2.5}$ was calculated according to an equation $\Delta E_{MP2.5} = E(MP2) + (1/2)E^{(3)}$, where $E^{(3)}$ is the third-order MP correlation energy correction. [e] A total energy calculated as the sum of the CBS energy and the correction term. [f] A Gibbs free energy of the complex obtained from the total energy (previous column) and the thermal correction to the Gibbs free energy calculated at the MP2/cc-pVDZ level at 298 K.

about 2 kcal/mol between the two H-bonded structures resembling a binding pattern between bases in DNA (WC-a and WC-b) and the two other H-bonded structures containing only two hydrogen bonds (R-a and R-b). Only these four structures can exist at room temperature according to calculated Gibbs free energies. The stacked structures and the T-shaped structures are less stable, both on the potential and free energy surface by at least 8 kcal/mol relative to the lowest energy structure. Furthermore, the IR frequencies do not match the experiment as will be discussed below.

WC-a is a straight equivalent of the WC structure in GC; the NH_2 and C═O groups are exchanged but the hydrogen bonding pattern and the geometry are entirely maintained. Thus, this structure has been proposed as a possible alternative base pair arrangement.[12] WC-b is an "inverted" version of WC-a in which the pyrimidine is flipped along the N3−C6 axis. An equivalent of this version does not occur in GC because it does not have a symmetrical H-bonded pattern (with two NH_2 groups on one molecule and two C═O groups on the other). Next in energy for GC is the reverse WC structure (RWC). This motif is not quite possible in the alternate base pair since there is no lone pair donor (oxygen) on the pyrimidine. However, there is an analogous motif in the form of R-a and its "inverted" version R-b, which are

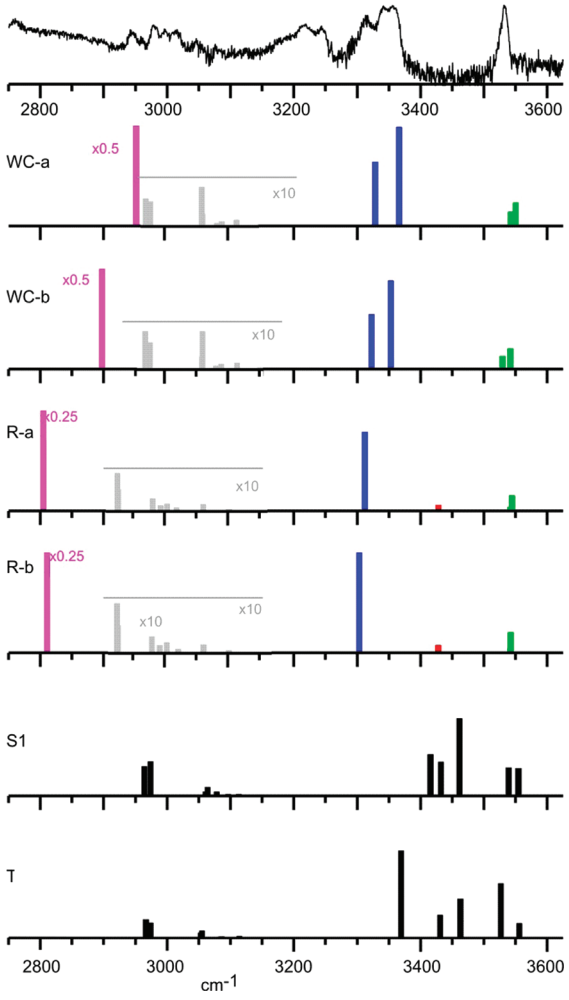

Figure 4. Experimental spectrum in the near-IR region (top panel, inverted to show a cross section of infrared absorption instead of depletion in the ion signal) and the calculated frequencies for the six lowest energy structures. Color coding indicates modes as follows: Green: asymmetric NH_2 stretches. Red: free symmetric NH_2 stretches. Blue: hydrogen bound symmetric NH_2 stretches. Purple: hydrogen bound NH stretch (displayed at reduced amplitude scale). Gray: CH modes (displayed at ×10 amplitude scale). The frequencies are all scaled with a factor of 0.957.

the next stable structures. Hoogsteen-type motifs are excluded in this case because the 7-methyl group blocks the necessary hydrogen bonding site.

dx.doi.org/10.1021/jp205831n |J. Phys. Chem. A XXXX, XXX, 000–000

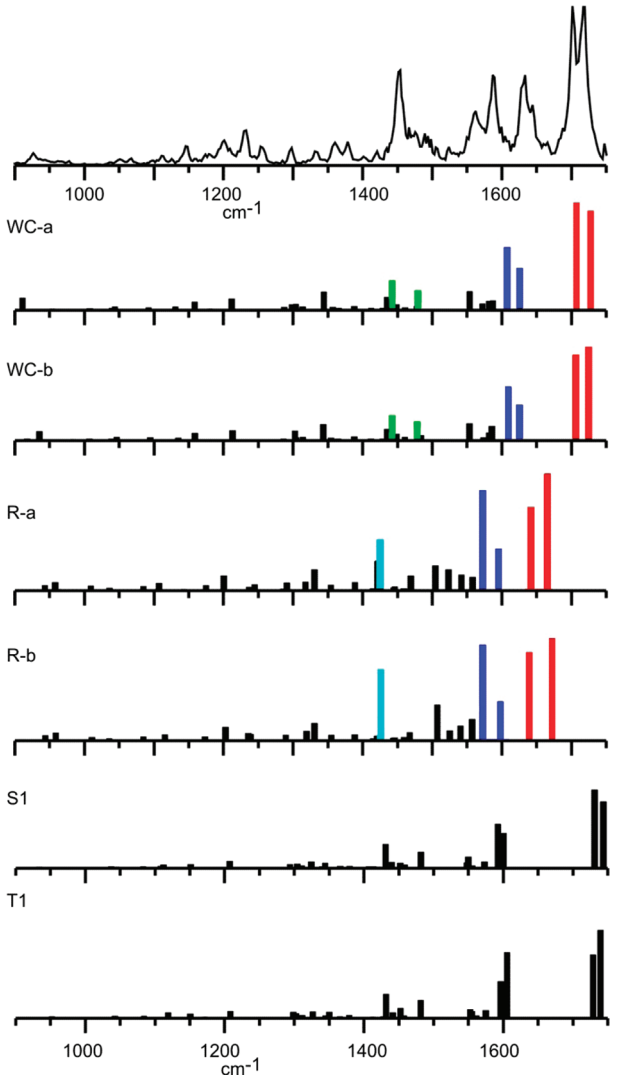

Figure 5. Experimental spectrum (top panel) and calculated frequencies (scaled by a factor of 0.957) for the four lowest energy structures. Color coding indicates modes as follows: Red: C═O stretches. Blue: free NH_2 scissors. Light blue: bound NH_2 scissors. Green: NH wag.

The UV two photon excitation spectrum is broad as shown in Figure 3. We verified that the broad nature of the spectrum is not an artifact of the dye laser intensity. We have obtained IR-UV double resonance spectra both in the near-IR (in Santa Barbara; Figure 4) and in the mid-IR (at FELIX; Figure 5). We have recorded the IR-UV hole burning spectrum at several UV probe wavelengths (33513 and 35475 cm^{-1} in Santa Barbara and 33557, 33450, and 33650 cm^{-1} at FELIX), resulting in the same IR spectrum independent of UV wavelength. As we will discuss below, four structures can be identified in the IR spectra. Therefore, although not all the possible UV wavelengths have been probed, our results suggest that the resonant two-photon ionization (R2PI) spectrum consists of overlapping spectra from at least these four cluster structures. The resulting congestion may partly explain the broad nature of the spectrum, although in the absence of additional spectral broadening our resolution should still be sufficient to resolve the individual vibronic peaks. Since we cannot select individual isomers by virtue of the probe wavelength, the IR spectra of all isomers are recorded simultaneously.

Figure 4 shows the IR-UV double resonance spectrum in the near-IR region. The experimental spectrum appears in the top panel, and is compared with calculated frequencies for the four lowest energy structures as well as one stacked and one T-shaped structure. The frequencies of S1 and S2 are very similar to each other, as are those for T1 and T2, so only one representative spectrum is shown for each of these structures. All frequencies are scaled with a factor 0.957. The color coding indicates modes as follows: asymmetric NH_2 stretches in green, free symmetric NH_2 stretches in red, hydrogen bound symmetric NH_2 stretches in blue, and the hydrogen bound NH stretches in purple. The latter is displayed at a reduced amplitude scale. The CH modes are shown in gray and displayed at a $\times 10$ amplitude scale.

For both the stacked structures and the T-shaped structures, the calculations predict strong bands in the 3400−3500 cm^{-1} range, due to the free symmetric NH_2 stretches and the free NH stretch. In this range, the experiment exhibits no absorption at all. Therefore we can exclude these types of structures. Additionally, we do not expect these structures to be present in the molecular beam due to their unfavorable stabilization energy.

The calculated frequencies of the four lowest energy structures are consistent with the experimental spectrum recorded in the near-IR region. The calculated asymmetric NH_2 stretches are all at about the same frequency of 3540 cm^{-1}, which fits well to the single peak at 3534 cm^{-1} in the experiment. The double peak at 3300−3340 cm^{-1} matches well with the hydrogen-bound symmetric NH_2 stretches, of which there are two in each of the WC structures and one in each of the R structures. The hydrogen bound NH stretch mode, present once in each structure, is the largest in amplitude and should be strongly broadened (which is reflected in broad feature in the spectrum). This leaves two questions. First, these data do not allow us to establish whether both the WC and the R structures are present. This question can be resolved by obtaining the IR spectrum of 24daP−TB in the mid-IR region, as shown below. Second, the double peak at 3200−3250 cm^{-1} does not match any of the calculated frequencies. This could indicate either another structure or, more probably, a larger than anticipated blue-shift on one of the modes, such as the H-bound symmetric NH_2 stretch of the R structures.

Figure 5 shows the results for the mid-IR region, with the data from the FELIX experiment. In this figure, the color coding signifies the following modes: the C═O stretches are presented in red, the NH_2 scissor modes are in blue, the hydrogen bonded NH_2 scissors are in light blue, and the NH wagging vibration is in green. For both the C═O stretching and NH_2 scissor modes, the asymmetric mode is the red most one, while the symmetric mode is shifted to the blue. Each of the sets of structures, WC and R, exhibits two pairs of strong peaks between 1500 cm^{-1} and 1750 cm^{-1}. However, unlike the case in the near-IR, these sets of peaks do not overlap, allowing us to determine that both sets of structures are present. If only the WC pair were present, we would expect just two strong doublets between 1550 and 1750 cm^{-1}. The fact that we observe more than two doublet features in this range thus leads us to conclude that the R structures are present as well. Once again the frequencies of the S- and T-type structures are inconsistent with experimental spectrum.

CONCLUSION

We investigated the IR spectroscopy and energetics of different isomers of the 24dAP−TB alternate base pair in the gas phase by IR-UV double resonance spectroscopy and ab initio calculations.

dx.doi.org/10.1021/jp205831n |J. Phys. Chem. A XXXX, XXX, 000–000

We observed the four lowest energy structures for this cluster in the molecular beam. These include a pair of structures with a hydrogen bonding pattern equivalent to the WC motif in GC. The other two structures are roughly equivalent to a RWC motif, although the full equivalent in this case is excluded by methyl-blocking of the relevant H-bonding location. The observation of the lowest energy WC-type structure is in marked contrast to the canonical base pairs, where in the gas phase we never observe this structure by nanosecond R2PI. The excited state lifetime is presumably long enough to allow efficient two photon ionization; however, the R2PI spectrum is also broad. The broad nature of the UV spectrum, in combination with the fact that it consists of overlapping spectra from different base pairs, makes it difficult to estimate actual lifetimes. We have initiated pump−probe experiments to measure excited state lifetimes as well as investigations of other alternate base pair combinations. In the case of the canonical GC pair, calculations by Sobolewski et al. show that the excited state lifetime is affected by rapid internal conversion via conical intersections.[5] This process depends on the shape of the excited state potential surfaces and is a strong function of the hydrogen-bonded structure, such that non-WC structures of the GC base pair can have long excited state life times, while the WC structure is short-lived. Future similar excited state dynamics calculations for the 24dAP−TB alternate base pair may further elucidate this issue.

■ ASSOCIATED CONTENT

Supporting Information. (Table S1) Structures found at the (B3LYP/6-311+G(d,p) level of theory. (Table S2) Frequencies (scaled by a factor of 0.957) and intensities for the two zitterionic isomers, shown in supplemental Table S1. This material is available free of charge via the Internet at http://pubs.acs.org.

■ AUTHOR INFORMATION

Corresponding Author

*E-mail: devries@chem.ucsb.edu.

■ ACKNOWLEDGMENT

This material is based upon work supported by the National Science Foundation under CHE-0911564. The skillful assistance of the FELIX staff is gratefully acknowledged. This work was a part of the research project No. Z40550506 of the Institute of Organic Chemistry and Biochemistry, Academy of Sciences of the Czech Republic and it was supported by Grants LC512 (Ministry of Education, Youth and Sports, Czech Republic) and No. IAA400550808 (Grant Agency of the Academy of Sciences of the Czech Republic).] MSdV thanks the Borchard Foundation for a Scholarship in Residence.

■ REFERENCES

(1) de Vries, M. S.; Hobza, P. *Annu. Rev. Phys. Chem.* **2007**, *58*, 585.
(2) Abo-Riziq, A.; Grace, L.; Nir, E.; Kabelac, M.; Hobza, P.; de Vries, M. S. *Proc. Natl. Acad. Sci. U.S.A.* **2005**, *102*, 20.
(3) Nir, E.; Kleinermanns, K.; Grace, L.; de Vries, M. S. *J. Phys. Chem. A* **2001**, *105*, 5106.
(4) Mons, M.; Piuzzi, F.; Dimicoli, I.; Gorb, L.; Leszczynski, J. *J. Phys. Chem. A* **2006**, *110*, 10921.
(5) Sobolewski, A. L.; Domcke, W.; Hättig, C. *Proc. Natl. Acad. Sci. U.S.A.* **2005**, *102*, 17903.
(6) Canuto, V. M.; Levine, J. S.; Augustsson, T. R.; Imhoff, C. L. *Nature* **1982**, *296*, 816.
(7) Sagan, C. *J. Theor. Biol.* **1973**, *39*, 195.
(8) Nir, E.; Hunig, I.; Kleinermanns, K.; de Vries, M. S. *Phys. Chem. Chem. Phys.* **2003**, *5*, 4780.
(9) Nir, E.; Janzen, C.; Imhof, P.; Kleinermanns, K.; de Vries, M. S. *Phys. Chem. Chem. Phys.* **2002**, *4*, 740.
(10) Nir, E.; Janzen, C.; Imhof, P.; Kleinermanns, K.; de Vries, M. S. *Phys. Chem. Chem. Phys.* **2002**, *4*, 732.
(11) Krueger, A. T.; Kool, E. T. *Chem. Biol.* **2009**, *16*, 242.
(12) Geyer, C. R.; Battersby, T. R.; Benner, S. A. *Structure* **2003**, *11*, 1485.
(13) Miyakawa, S.; Cleaves, H. J.; Miller, S. L. *Origins Life Evol. Biospheres* **2002**, *32*, 209.
(14) Rezac, J.; Fanfrlik, J.; Salahub, D.; Hobza, P. *J. Chem. Theory Comput.* **2009**, *5*, 1749.
(15) Hobza, P.; Sponer, J. *Chem. Rev.* **1999**, *99*, 3247.
(16) Frisch, M. J.; Trucks, G. W.; Schlegel, H. B.; Scuseria, G. E.; Robb, M. A.; Cheeseman, J. R.; Scalmani, G.; Barone, V.; Mennucci, B.; Petersson, G. A.; Nakatsuji, H.; Caricato, M.; Li, X.; Hratchian, H. P.; Izmaylov, A. F.; Bloino, J.; Zheng, G.; Sonnenberg, J. L.; Hada, M.; Ehara, M.; Toyota, K.; Fukuda, R.; Hasegawa, J.; Ishida, M.; Nakajima, T.; Honda, Y.; Kitao, O.; Nakai, H.; Vreven, T.; Jr., J. A., M.; Peralta, J. E.; Ogliaro, F.; Bearpark, M.; Heyd, J. J.; Brothers, E.; Kudin, K. N.; Staroverov, V. N.; Kobayashi, R.; Normand, J.; Raghavachari, K.; Rendell, A.; Burant, J. C.; Iyengar, S. S.; Tomasi, J.; Cossi, M.; Rega, N.; Millam, J. M.; Klene, M.; Knox, J. E.; Cross, J. B.; Bakken, V.; Adamo, C.; Jaramillo, J.; Gomperts, R.; Stratmann, R. E.; Yazyev, O.; Austin, A. J.; Cammi, R.; Pomelli, C.; Ochterski, J. W.; Martin, R. L.; Morokuma, K.; Zakrzewski, V. G.; Voth, G. A.; Salvador, P.; Dannenberg, J. J.; Dapprich, S.; Daniels, A. D.; Farkas, Ö.; Foresman, J. B.; Ortiz, J. V.; Cioslowski, J.; Fox, D. J. *Gaussian 09*, revision A.2; Gaussian, Inc.: Wallingford CT, 2009.
(17) Sponer, J.; Gabb, H. A.; Leszczynski, J.; Hobza, P. *Biophys. J.* **1997**, *73*, 76.
(18) Halkier, A.; Helgaker, T.; Jorgensen, P.; Klopper, W.; Koch, H.; Olsen, J.; Wilson, A. K. *Chem. Phys. Lett.* **1998**, *286*, 243.
(19) Pitonak, M.; Neogrady, P.; Cerny, J.; Grimme, S.; Hobza, P. *ChemPhysChem* **2009**, *10*, 282.
(20) Werner, H. J.; Eckert, F.; Hampel, C.; Heltzer, G.; Korona, T.; Lindh, R.; Lloyd, A. W.; McNicholas, S. J.; Manby, F. R.; Meyer, W.; Mura, M. E.; Knowles, P. J.; Nicklass, A.; Palmieri, P.; Pitzer, R.; Rauhut, G.; SchØtz, M.; Stoll, H.; Stone, A. J.; Tarroni, R.; Thorsteinsson, T.; Amos, R. D.; Bernhardsson, A.; Berning, A.; Celani, P.; Cooper, D. L.; Deegan, M. J. O.; Dobbyn, A. J. *MOLPRO 2010: A Package of ab Initio Programs*, 2010.
(21) Meijer, G.; Devries, M. S.; Hunziker, H. E.; Wendt, H. R. *Appl. Phys. B: Photophys. Laser Chem.* **1990**, *51*, 395.
(22) Oepts, D.; Vandermeer, A. F. G.; Vanamersfoort, P. W. *Infrared Phys. Technol.* **1995**, *36*, 297.
(23) von Helden, G.; van Heijnsbergen, D.; Meijer, G. *J. Phys. Chem. A* **2003**, *107*, 1671.
(24) Rijs, A. M.; Kay, E. R.; Leigh, D. A.; Buma, W. J. *J. Phys. Chem. A* **2011**, DOI: 10.1021/jp200909v.
(25) Krishnan, R.; Binkley, J. S.; Seeger, R.; Pople, J. A. *J. Chem. Phys.* **1980**, *72*, 650.